COMMUNICATION

# Supramolecular capture of highly polar amidosquaraine dye in water with nanomolar affinity and large turn-on fluorescence †

Received 00th January 20xx,
Accepted 00th January 20xx

DOI: 10.1039/x0xx00000x

Madushani Dharmarwardana, Janel M. Dempsey, Sasha Padilla-Coley, Tia S. Jarvis, Kejia Shi, Kirk M. Atkinson, Bradley D. Smith*

**A supramolecular dye-capture system comprised of anionic amidosquaraine guest and macrocyclic tetralactam host exhibits nanomolar affinity and "turn on" visible fluorescence. Utility is demonstrated with a new fluorescent assay for liposome leakage induced by the biomedically important enzyme phospholipase $A_2$.**

An active research topic in modern host/guest chemistry is the development of supramolecular dye-capture systems for use in various diagnostic and imaging applications.[1] [2] [3] The desired functional properties are determined primarily by the specific performance demands of the application and include supramolecular and physical parameters such as the thermodynamics and kinetics of the host/guest association, solubility in the operating media, and propensity of the molecules to self-aggregate.[4] [5] If the output signal is fluorescence, then there are several photophysical parameters to optimize such as the emission wavelength and the choice of fluorescence output paradigm which can either be intensiometric or ratiometric detection.[6]

Roughly speaking, there are three main classes of synthetic supramolecular dye-capture systems: metal coordination complexes that bind a dye by direct metal ligation,[7] bowl-shaped host molecules that attract dyes using favorable electrostatic effects,[8] or macrocylic hosts that encapsulate a dye and form an inclusion complex.[9] [10] Performance in real-world biomedical samples is often degraded by the competing ligands or ions that are present in physiological media.[11] Some of the classic macrocylic hosts, such as cyclodextrins and cucurbiturils, have very high affinity for specific hydrophobic guests whose molecular shape matches the host cavity,[9] but most fluorescent dyes do not have the correct complementary shape and association constants ($K_a$) are usually <$10^7$ $M^{-1}$.[12] Some researchers have developed guest-dye conjugates for strong supramolecular capture,[4] [13] but the use of guest-dye conjugates has inherent technical drawbacks that can degrade the fluorescence response, such as undesired conjugate self-aggregation, or off-target association with biomembranes. Moreover, the capture host only interacts with the guest component of a guest-dye conjugate and does not modulate the fluorescence of the appended dye component. A high-affinity dye-capture system that reports binding by "turning on" the dye fluorescence signal is advantageous for imaging and sensing because the background signal is inherently low, but at present, the combination of high affinity and "turn on" fluorescence can only be achieved using a host molecule that has been synthetically modified to permit fluorescence energy transfer.[14] [15] [16]

A few years ago, an opportunity arose to address this problem when we discovered that water-soluble, fluorescent squaraine dyes, such as **SQ1**, can be encapsulated with high affinity inside preorganized tetralactam host molecules, such as **M1** (Scheme 1).[17] [18] The very high $K_a$ values ($10^7$ - $10^{11}$ $M^{-1}$) are due to a synergistic combination of stabilizing hydrogen bonds between the squaraine oxygen atoms and the inward directed tetralactam NH residues, and hydrophobic squaraine stacking against the host anthracene sidewalls.[19] Squaraine encapsulation induces a 20-30 nm red shift in the dye's deep-red absorption and emission maxima bands and a small increase in fluorescence quantum yield. More recently, we discovered

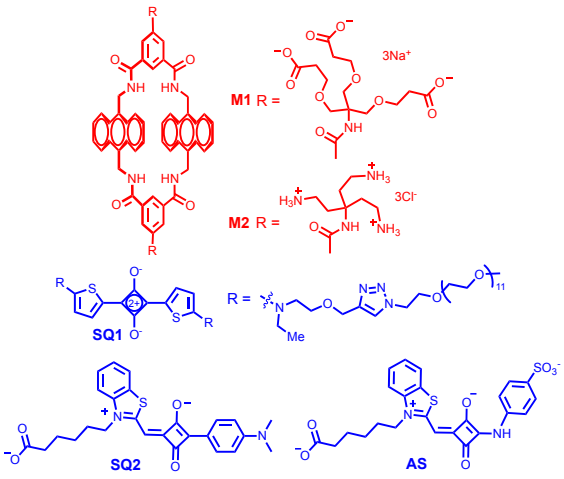


**Scheme 1**. Chemical structures of macrocycles and squaraine derivatives used in the study.

*Department of Chemistry and Biochemistry, 251 Nieuwland Science Hall, University of Notre Dame, Notre Dame, IN 46556, USA*
**Email: smith.115@nd.edu*
†Electronic Supplementary Information (ESI) available: Compound synthesis, supplementary figures, movies of 3D structures. See DOI: 10.1039/x0xx00000x

that tetralactam encapsulation of unsymmetrical, solvatochromatic squaraine dyes such as **SQ2** produces a significantly greater ~80 nm red-shift in squaraine absorption that translates into a very large increase in squaraine emission intensity.[20] While the "turn-on" fluorescence exhibited by the **M1**/**SQ2** pair is very impressive there are two supramolecular drawbacks: one is a moderate $K_a$ value of $10^7$ $M^{-1}$ which is not strong enough for demanding sensing applications, and the other is the moderately hydrophobic structure of **SQ2** which can potentially favor undesired off-target association events that decrease imaging or sensing performance. Thus, the aim of this present study was to mitigate these two problems by finding a new highly polar squaraine guest molecule that can be encapsulated by a tetralactam host with very high affinity and "turn on" fluorescence.

Our previous success using the concept of guest "back-folding" to improve the affinity of squaraine/tetralactam pairs led us to consider highly polar squaraine derivatives with bent molecular shapes as potential guests.[18 21] The literature on squaric acid derivatives includes a wide range of squarates,[22] squaramides,[23] and unsymmetrical squaraines,[24] but we were drawn to a relatively unexplored structural family that we call amidosquaraines, with two aryl substituents on a squarate ring in a 1,3-orientation; one ring connected by a C-C bond and the other ring attached by C-N bond.[25 26] As described below, a molecular model suggested that the novel amidosquaraine, **AS**, could be encapsulated as a guest within the cavity of a tetralactam host and simultaneously "fold-back" to make favorable non-covalent contacts with the macrocycle exterior surface.

The first goal of the project was to make **AS** and this was achieved using the straightforward synthetic method described in the ESI. Amidosquaraine **AS** is highly water soluble and excitation of its absorption maxima band at 510 nm produces very weak fluorescence (Figure S14). Titration experiments monitored the changes in **AS** absorption and emission bands induced by addition of hexa-anionic tetralactam **M1**. As shown in Figure S14, encapsulation of **AS** by **M1** macrocycle produced a 35 nm red shift in the **AS** absorption maxima band and ~25-fold increase in the fluorescence intensity. The large enhancement of **AS** fluorescence is attributed to restricted rotation of the squarate C-N bond when the dye is inside the macrocyclic host, which inhibits excited state relaxation by non-radiative pathways.[20 27] NMR spectra of the **M1⊃AS** complex supported this structural picture.§ Fluorescence titration experiments determined $K_a$ = (2.2 ± 0.7) × $10^7$ $M^{-1}$ in water which is remarkably high for an equilibrium that involves encapsulation of a bis-anionic guest (**AS**) by a hexa-anionic host (**M1**).

The repulsive electrostatic effect was converted into an attractive interaction by synthesizing the new tetralactam, **M2**, with six appended cationic ammonium groups (see ESI for synthetic details).[28] Encapsulation of **AS** by hexa-cationic **M2** was studied by titration experiments that produced large changes in **AS** absorption and emission bands. The representative data in Figure 1 shows that addition of **M2** produced ~35 nm red shift in **AS** absorption and ~35-fold increase in **AS** fluorescence intensity. Moreover, the fluorescence enhancement is easily discerned by the naked eye. The "turn-on" fluorescence enabled fluorescence titration experiments that monitored the increase in fluorescence at 575 nm due to the formation of **M2⊃AS**. Fitting the curve to a 1:1 binding model suggested that the association constant $K_a$ was ≥ 2 × $10^9$ $M^{-1}$ (Figure 1b, insert). The uncertainty for this remarkably strong association constant is high because the value is at the analytical limit of the fluorescence titration method. Therefore, the enhanced affinity for **AS** was confirmed by conducting an independent guest-selection experiment using squaraine **SQ2** as a competing guest in the same solution of phosphate buffered saline (PBS). A preliminary measurement determined $K_a$ = (6.6 ± 3.4) × $10^6$ $M^{-1}$) for encapsulation of **SQ2** by **M2** in pH 7.4, PBS at 25 °C (Figure S15) to give a complex that emits at 690 nm.[20] The basis of the guest-selection experiment is selective fluorescence energy transfer from the excited anthracene sidewalls of host **M2** to the encapsulated guest (**SQ2** or **AS**).[21] The fluorescence profiles in Figure 2b show that the complex **M2⊃AS** emission at 575 nm is easily distinguished from the **M2⊃SQ2** emission at 690 nm. As explained by the cartoon summary in Figure 2a, adding one molar equivalent of **M2** to a 1:1 binary mixture of **AS** and **SQ2** in PBS produced preferential encapsulation of the higher-affinity guest **AS**, whereas, adding five molar equivalents of **M2** to the 1:1 binary mixture produced host encapsulation of both guests.

The independent data are consistent and indicate that $K_a$ for formation of **M2⊃AS** is about two orders of magnitude higher than the $K_a$ value for formation of **M2⊃SQ2**. In order to rationalize the large affinity enhancement, a set of molecular modelling computations were conducted, and shown in Figure 2c is a low low-energy structure of the non-covalent **M2⊃AS** complex with the encapsulated **AS** adopting a *trans* conformation.‡ The encapsulated **AS** guest within the **M2⊃AS** complex "folds-back" and forms favorable hydrophobic stacking contacts with the isophthalamide bridging units of the surrounding **M2** macrocycle.§ [18 21] There is also ion-paring between the anionic carboxylate and sulfonate groups at each end of the **AS** guest and the three cationic ammonium groups on each dendritic chain appended to the ends of **M2**.[29] In contrast, guest **SQ2** lacks a sulfonate group and it is unable to "fold-back" like **AS**. Thus, there is a lower number of ion-pairing

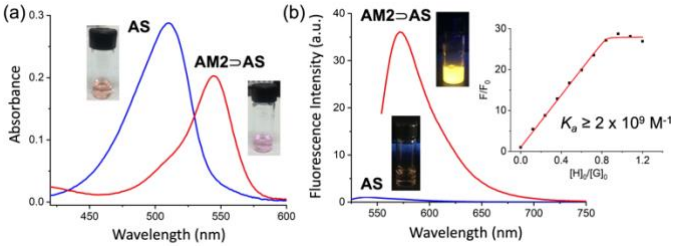


**Figure 1.** (a) Absorption spectra for **AS** (blue) and **M2⊃AS** (red). (b) Emission spectra for **AS** (blue, ex: 510 nm) and **M2⊃AS** (red, ex: 545 nm). In all cases, 10 μM in water at 25 °C. Insert: Representative titration isotherm with fitting to 1:1 association model.

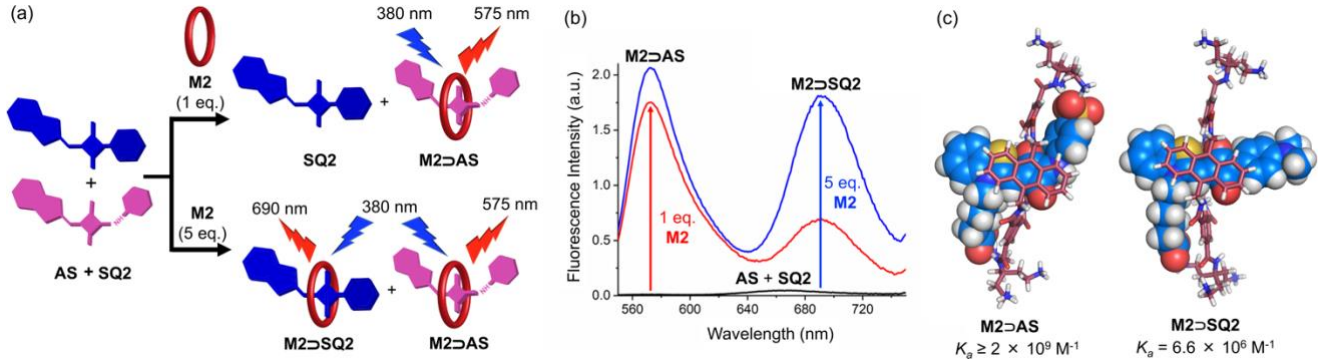


**Figure 2.** (a) Cartoon explaining the guest-selective encapsulation experiment. Addition of one molar equivalent (1 eq.) of **M2** to a 1:1 binary mixture of **AS** and **SQ2** selectively forms **M2⊃AS**, whereas addition of five molar equivalents (5 eq.) of **M2** produces encapsulation of both guests. (b) Fluorescence profile for a binary mixture of 1:1 **SQ2** and **AS** (2 μM each) with 380 nm excitation. Black curve: **M2** is absent. Red curve: after one molar equivalent of **M2** is added. Blue curve: after five molar equivalents of **M2** is added. At 25 °C in PBS, pH 7.4. (c) Molecular models of energy-minimized complexes computed using the PM7 method.

and hydrophobic stacking interactions to stabilize the **M2⊃SQ2** complex (Figure 2c).

To demonstrate the utility of **M2**/**AS** as a dye-capture system, we incorporated the pair within a novel liposome leakage assay (Figure 3a). Liposome leakage assays are used often in biomembrane research, and triggered liposome release is a common functional strategy in drug delivery and diagnostics.[30] [31] Fluorescent liposome leakage assays are convenient procedures and a very common method is to entrap a fluorescent dye, such as carboxyfluorescein, at a very high, self-quenching concentration (typically 50 mM), or similarly entrap a dye/quencher pair.[31] In these cases, liposome leakage releases diluted "unquenched" dye into the aqueous exterior and the assay produces an increase in fluorescence intensity. While technically straightforward, the very high dye concentrations are a source of mechanistic uncertainty about the leakage process. For example, fluorescent dyes are often self-aggregated at high concentration in water, which means there is ambiguity about the size of the molecular species that permeates the liposome bilayer. In addition, it is well-established that many water-soluble fluorophores interact with bilayer membranes,[32] and a very high dye concentration inside a liposome increases the likelihood of bilayer membrane disrupting effects.[33] Combined, these concerns highlight the need for new liposome leakage assays that use a relatively low concentration of entrapped highly polar fluorescent marker.[16]

We focused on a fluorescent assay that reported liposome leakage induced by phospholipase $A_2$ ($PLA_2$), a calcium-dependent esterase enzyme that disrupts membranes by hydrolyzing the fatty ester group at the *sn*-2 position of glycerophospholipids (Figure S17). Assays that report $PLA_2$-induced liposome leakage are used often by different types of researchers developing: $PLA_2$-inhibitors as drug candidates,[34] nanocapsules for $PLA_2$-triggered drug release,[35] and diagnostic sensors of $PLA_2$ levels in biomedical samples.[36] Evidence that **M2**/**AS** is effective within a $PLA_2$-induced liposome leakage assay was gained by conducting experiments using POPC (1-palmitoyl-2-oleoyl-*sn*-glycero-3-phosphocholine) liposomes containing 500 μM of **AS** (POPC@**AS**). In the absence of **M2**, $PLA_2$-induced leakage of **AS** from the liposomes produced little change in sample fluorescence, but in the presence of **M2** (10 μM) there was a 30-fold fluorescence increase due to capture of the leaked **AS** (Figure S18)**.** Figure 3b shows the $PLA_2$-induced leakage of POPC@**AS** liposomes over time, along with representative photographs of illuminated cuvettes revealing a dramatic "turn on" in visible fluorescence that is easily discerned by the naked eye. The leakage rate matched an analogous liposome assay based on carboxyfluorescein leakage, strongly suggesting that $PLA_2$-mediated hydrolysis and membrane disruption is the common rate determining step (Figure S19). The results indicate clearly that fluorescent liposome assays using **M2**/**AS** are well suited for point-of-care diagnostics or high-throughput screening technologies.

In summary, the molecular design concept of guest back-folding has been successfully applied to increase the affinity of a supramolecular dye-capture system, and a tangible outcome of this work is a new liposome leakage assay that exploits the nanomolar affinity and "turn on" visible fluorescence of **M2**/**AS**. While macrocyclic tetralactam hosts are known to bind some of the small biomolecules that are present in complex biological media, the moderate affinities are not likely to inhibit the

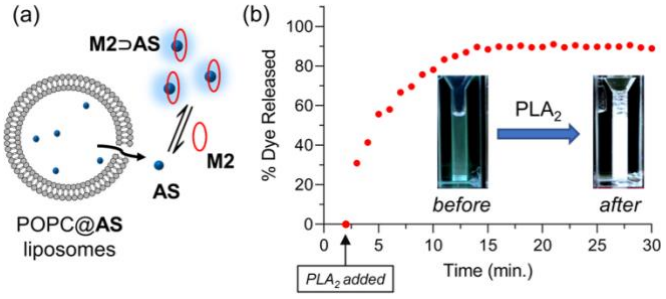


**Figure 3.** (a) Schematic summary of the liposome leakage assay. (b) Leakage profile for POPC@**AS** liposomes treated with $PLA_2$. Representative photographs of cuvettes illuminated with UV light, showing that liposome leakage can be visualized by the naked eye. External solution: 10 mM HEPES, 3 mM $CaCl_2$ (pH 7.4) at 25 °C.

performance of **M2**/**AS**.[37] We expect that **M2**/**AS**, and next-generation bioconjugates, will be useful for a multitude of affinity-based applications such as bioconjugate self-assembly, surface immobilization, and fluorescence sensing.[1] We are grateful for funding support from the US NIH (R35GM136212) and NSF (CHE1708240).

## Conflicts of interest

There are no conflicts to declare.

## Notes and references

§The limited water solubility of the **M2⊃AS** complex prevented NMR studies. However, the more water-soluble **M1⊃AS** complex was amenable to characterization by 1D and 2D NMR, and the data (described in Section 4 of the Electronic Supplementary Information) supports the structural picture in Figure 2c.

‡ The same non-covalent interactions are present in a similar energy-minimized structure of the **M2⊃AS** complex with the **AS** guest in a *cis* conformation (Figure S20).


1 W. Liu, S. K. Samanta, B. D. Smith and L. Isaacs, *Chem. Soc. Rev.*, 2017, **46**, 2391–2403.
2 H. B. Cheng, Y. Li, B. Z. Tang and J. Yoon, *Chem. Soc. Rev.*, 2020, **49**, 21–31.
3 T. L. Mako, J. M. Racicot and M. Levine, *Chem. Rev.*, 2019, **119**, 322–477.
4 C. J. Addonizio, B. D. Gates and M. J. Webber, *Bioconjugate Chem*., 2021, DOI:10.1021/acs.bioconjchem.1c00326.
5 C. L. Schreiber and B. D. Smith, *Nat. Rev. Chem.*, 2019, **3**, 393–400.
6 S. Sinn, J. Krämer and F. Biedermann, *Chem. Commun.*, 2020, **56**, 6620–6623.
7 I. A. Rather and R. Ali, *Org. Biomol. Chem.*, 2021, **19**, 5926–5981.
8 M. A. Romero, P. Mateus, B. Matos, Á. Acunã, L. Garciá-Rió, J. F. Arteaga, U. Pischel and N. Basílio, *J. Org. Chem.*, 2019, **84**, 10852–10859.
9 J. Murray, K. Kim, T. Ogoshi, W. Yao and B. C. Gibb, *Chem. Soc. Rev.*, 2017, **46**, 2479–2496.
10 S. Sinn, E. Spuling, S. Bräse and F. Biedermann, *Chem. Sci.*, 2019, **10**, 6584–6593.
11 M. A. Beatty and F. Hof, *Chem. Soc. Rev.*, 2021, **50**, 4812–4832.
12 R. N. Dsouza, U. Pischel and W. M. Nau, *Chem. Rev.*, 2011, **111**, 7941–7980.
13 A. Som, M. Pahwa, S. Bawari, N. Das Saha, R. Sasmal, M. S. Bosco, J. Mondal and S. S. Agasti, *Chem. Sci.*, 2021, **12**, 5484–5494.
14 M. Li, S. Kim, A. Lee, A. Shrinidhi, Y. H. Ko, H. G. Lim, H. H. Kim, K. B. Bae, K. M. Park and K. Kim, *ACS Appl. Mater. Interfaces*, 2019, **11**, 43920–43927.
15 R. Sasmal, N. Das Saha, M. Pahwa, S. Rao, D. Joshi, M. S. Inamdar, V. Sheeba and S. S. Agasti, *Anal. Chem.*, 2018, **90**, 11305–11314.
16 B. Gong, B. K. Choi, J. Y. Kim, D. Shetty, Y. H. Ko, N. Selvapalam, N. K. Lee and K. Kim, *J. Am. Chem. Soc.*, 2015, **137**, 8908–8911.
17 E. M. Peck, W. Liu, G. T. Spence, S. K. Shaw, A. P. Davis, H. Destecroix and B. D. Smith, *J. Am. Chem. Soc.*, 2015, **137**, 8668–8671.
18 W. Liu, A. Johnson and B. D. Smith, *J. Am. Chem. Soc.*, 2018, **140**, 3361–3370.
19 J. Dong and A. P. Davis, *Angew. Chem. Int. Ed.*, 2021, **60**, 8035–8048.
20 T. S. Jarvis and B. D. Smith, *Supramol. Chem.*, 2019, **31**, 140–149.
21 J. M. Dempsey, C. Zhai, H. H. Mcgarraugh, C. L. Schreiber, S. E. Stoffel, A. Johnson and B. D. Smith, *Chem. Commun.*, 2019, **55**, 12793–12796.
22 S. L. Kitson, *J. Diagnostic Imaging Ther.*, 2017, **4**, 35–75.
23 L. A. Marchetti, L. K. Kumawat, N. Mao, J. C. Stephens and R. B. P. Elmes, *Chem*, 2019, **5**, 1398–1485.
24 S. Khopkar, M. Jachak and G. Shankarling, *Dye. Pigment.*, 2019, **161**, 1–15.
25 C. G. Collins, J. M. Baumes and B. D. Smith, *Chem. Commun.*, 2011, **47**, 12352–12354.
26 G. Xia and H. Wang, *J. Photochem. Photobiol. C Photochem. Rev.*, 2017, **31**, 84–113.
27 Y. Ohsedo, K. Saruhashi and H. Watanabe, *Dye. Pigment.*, 2015, **122**, 134–138.
28 T. S. Carter, T. J. Mooibroek, P. F. N. Stewart, M. P. Crump, M. C. Galan and A. P. Davis, *Angew. Chem. Int. Ed.*, 2016, **55**, 9311–9315.
29 H. Destecroix, C. M. Renney, T. J. Mooibroek, T. S. Carter, P. F. N. Stewart, M. P. Crump and A. P. Davis, *Angew. Chem. Int. Ed.*, 2015, **54**, 2057–2061.
30 R. R. C. New, *Liposomes : a practical approach*, IRL Press ; Oxford University Press, Oxford; New York; New York, 1990.
31 G. Nasr, H. Greige-Gerges, A. Elaissari and N. Khreich, *Int. J. Pharm.*, 2020, **580**, 119198.
32 L. D. Hughes, R. J. Rawle and S. G. Boxer, *PLoS One*, 2014, **9**, e87649.
33 Z. Zhang, D. Yomo and C. Gradinaru, *Biochim. Biophys. Acta - Biomembr.*, 2017, **1859**, 1242–1253.
34 A. Nikolaou, M. G. Kokotou, S. Vasilakaki and G. Kokotos, *Biochim. Biophys. Acta - Mol. Cell Biol. Lipids*, 2019, **1864**, 941–956.
35 M. Mumtaz Virk and E. Reimhult, *Langmuir*, 2018, **34**, 395–405.
36 R. Chapman, Y. Lin, M. Burnapp, A. Bentham, D. Hillier, A. Zabron, S. Khan, M. Tyreman and M. M. Stevens, *ACS Nano*, 2015, **9**, 2565–2573.
37 D. Van Eker, S. K. Samanta and A. P. Davis, *Chem. Commun.*, 2020, **56**, 9268–9271.


 